

This is the peer reviewed version of the following article:

Enzyme-like Supramolecular Iridium Catalysis Enabling C–H Bond Borylation of Pyridines with meta-Selectivity / Trouve, J.; Zardi, P.; Al-Shehimi, S.; Roisnel, T.; Gramage-Doria, R.. - In: ANGEWANDTE CHEMIE. INTERNATIONAL EDITION. - ISSN 1433-7851. - 60:33(2021), pp. 18006-18013. [10.1002/anie.202101997]

*Terms of use:*

The terms and conditions for the reuse of this version of the manuscript are specified in the publishing policy. For all terms of use and more information see the publisher's website.

13/05/2026 01:31

(Article begins on next page)



**HAL**  
open science

# Enzyme-Like Supramolecular Iridium Catalysis Enabling C-H Bond Borylation of Pyridines with meta-Selectivity

Rafael Gramage-Doria, Jonathan Trouvé, Paolo Zardi, Shaymaa Al-Shehimi,  
Thierry Roisnel

► **To cite this version:**

Rafael Gramage-Doria, Jonathan Trouvé, Paolo Zardi, Shaymaa Al-Shehimi, Thierry Roisnel. Enzyme-Like Supramolecular Iridium Catalysis Enabling C-H Bond Borylation of Pyridines with meta-Selectivity. *Angewandte Chemie International Edition*, 2021, 60 (33), pp.18006-18013. 10.1002/anie.202101997 . hal-03193308

**HAL Id: hal-03193308**

**<https://hal.archives-ouvertes.fr/hal-03193308>**

Submitted on 15 Sep 2021

**HAL** is a multi-disciplinary open access archive for the deposit and dissemination of scientific research documents, whether they are published or not. The documents may come from teaching and research institutions in France or abroad, or from public or private research centers.

L'archive ouverte pluridisciplinaire **HAL**, est destinée au dépôt et à la diffusion de documents scientifiques de niveau recherche, publiés ou non, émanant des établissements d'enseignement et de recherche français ou étrangers, des laboratoires publics ou privés.

## RESEARCH ARTICLE

Enzyme-Like Supramolecular Iridium Catalysis Enabling C-H Bond Borylation of Pyridines with *meta*-Selectivity

Jonathan Trouvé, Paolo Zardi, Shaymaa Al-Shehimi, Thierry Roisnel, and Rafael Gramage-Doria\*

**Abstract:** The use of secondary interactions between substrates and catalysts is a promising strategy to discover selective transition metal catalysts for atom-economy C-H bond functionalizations. Unfortunately, the most powerful catalysts are still found *via* trial-and-error screening due to the low association constants between the substrate and the catalyst in which small stereo-electronic modifications in the catalyst (and/or the substrate) can lead to completely different reactivity patterns. In order to circumvent these limitations and to increase the level of reactivity prediction in this type of important reactions, we report herein a supramolecular catalyst harnessing Zn<sup>II</sup>-N interactions that bind to pyridine-like substrates as tight as it could be found in some enzymes. Furthermore, the distance and spatial geometry between the catalytically active site and the substrate binding site is ideal to target unprecedented *meta*-selective iridium-catalyzed C-H bond borylations with enzymatic Michaelis-Menten kinetics, besides unique substrate-selectivity and dormant reactivity patterns.

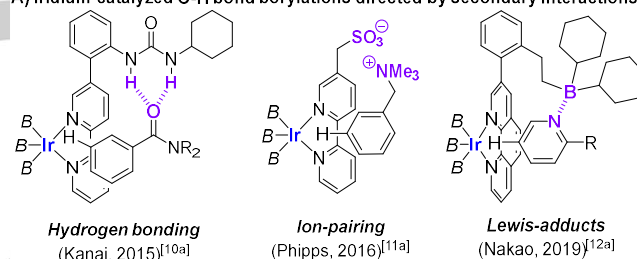
## Introduction

In the last three decades, C-H bond functionalizations enabled by transition metal catalysts have shown a remarkable impact in the advancement of chemical synthesis due to high atom- and step-economy it represents.<sup>[1]</sup> Besides substrates with a biased reactivity<sup>[2]</sup> or controlled by metal-directing groups,<sup>[3]</sup> the reactivity at inherently unreactive sites is of paramount importance to access new chemical dimensions. To meet this challenge, a standard approach deals with extensive fine-tuning of the catalyst first coordination sphere with different stereo-electronic modifications<sup>[4]</sup> or to introduce multiple catalytic cycles.<sup>[5]</sup> Although useful, substantial costs and efforts need to be undertaken to trial-and-error studies to search for the optimal catalytic system.

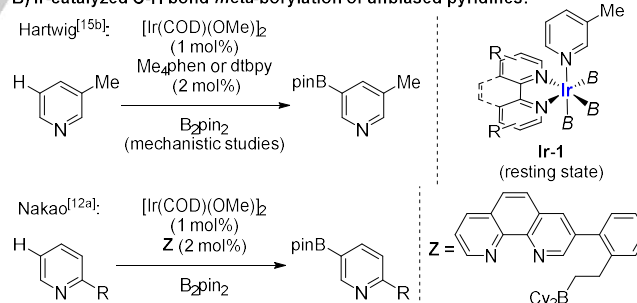
On the other hand, enzymes, Nature's catalysts, exploit alternative approaches to control chemical reactivity.<sup>[6]</sup> Importantly, they incorporate a number of kinetically reversible interactions in the second coordination sphere of the active site to stabilize key transition states.<sup>[7]</sup> For chemists, this has been a source of inspiration to mimic in abiological catalysis.<sup>[8]</sup> As such, different strategies have been developed to design transition metal catalysts incorporating remote functionalities to pre-organize substrates in a specific geometry to access unprecedented C-H bond functionalizations.<sup>[9]</sup> In this context, the incorporation of hydrogen bonding,<sup>[10]</sup> ion-pairing<sup>[11]</sup> or Lewis-adducts formation,<sup>[12]</sup> respectively, to transition metal catalysts

has emerged as promising approaches to control the regio-selectivity in iridium-catalyzed C-H bond borylation reactions (**Figure 1A**).<sup>[13]</sup> Borylated products are relevant as they can straightforward be engaged in state-of-the-art carbon-carbon and carbon-heteroatom bond forming process.<sup>[14]</sup> Unfortunately, the predictability of these catalytic systems is still poor rationalized, basically due to the low association constants between the substrate and the catalyst, generally with  $K < 10^2 \text{ M}^{-1}$ .<sup>[10-12]</sup> Consequently, small modifications in the commonly-used bipyridine-derived ligand and/or the substrate can lead to a complete lack of reactivity or absence of selectivity.<sup>[10-12]</sup> Precisely, we aimed at circumventing the poor reactivity of pyridine derivatives at *meta* position.<sup>[15a]</sup> Iridium-catalyzed C-H bond borylations typically occur at the *meta* position of pyridine derivatives when bulky substituents are present in the *ortho* site in order to prevent the undesired coordination of the pyridine nitrogen lone pair to the iridium catalyst, which gives unproductive and unselective catalysis (**Figure 1B**).<sup>[12a,15b]</sup>

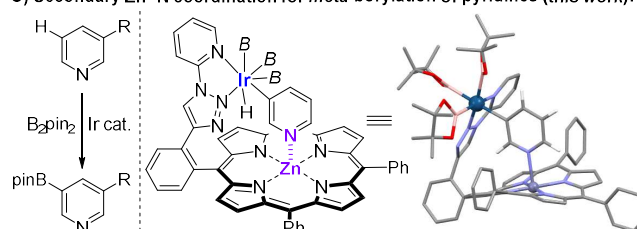
A) Iridium-catalyzed C-H bond borylations directed by secondary interactions:



B) Ir-catalyzed C-H bond *meta*-borylation of unbiased pyridines:



C) Secondary Zn<sup>II</sup>-N coordination for *meta*-borylation of pyridines (*this work*):



[a] J. Trouvé, Dr. P. Zardi, S. Al-Shehimi, Dr. T. Roisnel, Dr. R. Gramage-Doria  
Univ Rennes, CNRS, ISCR-UMR6226, F-35000 Rennes, France  
E-mail: rafael.gramage-doria@univ-rennes1.fr

Supporting information for this article is given via a link at the end of the document. ((Please delete this text if not appropriate))

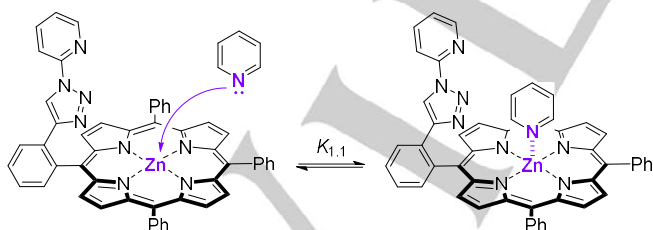
**Figure 1.** Overview of regio-selective iridium-catalyzed C-H bond borylation reactions guided by secondary interactions and issues encountered in pyridine *meta*-C-H bond reactivity (state-of-the art vs present work). **B** = (pinacolato)boron.  $\text{B}_2\text{pin}_2$  = bis(pinacolato)diboron. COD = 1,5-cyclooctadiene.

## RESEARCH ARTICLE

To overcome these challenges, we anticipated that a geometrically-constrained iridium catalyst featuring a relatively strong pyridine-to-catalyst interaction may increase the activity and selectivity for C-H bond borylation reactions. Herein, we present a rationally-designed supramolecular iridium catalyst exhibiting strong affinity for pyridine derivatives ( $K > 10^4 \text{ M}^{-1}$ ) by means of kinetically labile  $\text{Zn}\cdots\text{N}$  coordination (**Figure 1C**).<sup>[16]</sup> Due to the perfect geometry and ideal atom-precise distance between the active site and the substrate-recognition site, only *meta*-borylated pyridines were obtained (**Figure 1C**). In addition, the catalytic system displayed enzyme-like features such as Michaelis-Menten kinetics and substrate selectivity. Applications to five-membered nitrogen-containing heterocycles and dormant reactivity are also disclosed.

## Results and Discussion

Semi-empirical molecular modelling (PM3-level) showed that the geometry of ligand **L** (**Scheme 1** and **Figure 1C**) as well as the distance between the zinc(II)-porphyrin fragment (*the substrate binding site*) and the iridium *N,N*-chelating motif (*the potentially catalytically active site*) in the periphery is suitable to accommodate pyridine substrates with selective activation at the *meta*-C-H bond site.<sup>[17]</sup> In addition, the restricted motion between the *N,N*-chelating motif and the zinc(II)-porphyrin backbone will increase the rigidity of the system by keeping the peripheral iridium active site just above the zinc(II)-porphyrin plane. With this in mind, the targeted supramolecular ligand **L** was readily synthesized in a four-step reaction sequence starting from commercially available chemicals (see **Scheme S1**).<sup>[18]</sup> As expected, ligand **L** is in keeping with a  $C_s$ -symmetrical molecule according to NMR spectroscopy studies.<sup>[18]</sup>  $^1\text{H}$  NMR and UV-vis binding studies established the ability of **L** to interact with pyridine as the model substrate with an association constant of  $K_{1,1} = 5.7 \times 10^4 \pm 1.5 \text{ M}^{-1}$  at room temperature (**Scheme 1**, see **Figures S1-S3**).<sup>[18,19]</sup> Notably, this substrate-to-catalyst binding is as tight as it can be found in some enzymes.<sup>[20]</sup> The binding of pyridine to **L** was also evidenced by  $^1\text{H}$  NMR studies at temperatures up to 90 °C and by DOSY experiments that showed that the up-field shifted proton signals belonging to the pyridine diffused together with those corresponding to **L** (see **Figures S4-S7**).<sup>[18]</sup>



**Scheme 1.** Binding of pyridine to **L** via kinetically labile  $\text{Zn}\cdots\text{N}$  coordination.

Moreover, single crystals suitable for X-ray diffraction studies were obtained from a solution containing **L** and pyridine in an equimolar ratio (**Figure 2**, left).<sup>[21]</sup> As anticipated, the nitrogen atom from pyridine binds to the zinc(II) center of **L**. Gratifyingly, the coordinating arm of **L** stands in the same face as the substrate with a volumetric space between both motifs enough

to accommodate a catalytically active iridium center. Analogously single crystals with a potential substrate, *N*-methylimidazole, were also obtained and analysed by X-ray diffraction studies (**Figure 2**, right). As expected, the non-methylated nitrogen atom (N1) from the substrate was bound to the zinc(II) center from **L**. The binding of *N*-methylimidazole to **L** via  $\text{Zn}\cdots\text{N}$  interaction was also corroborated in solution by  $^1\text{H}$  NMR spectroscopy studies (see **Figure S13**).<sup>[18]</sup>

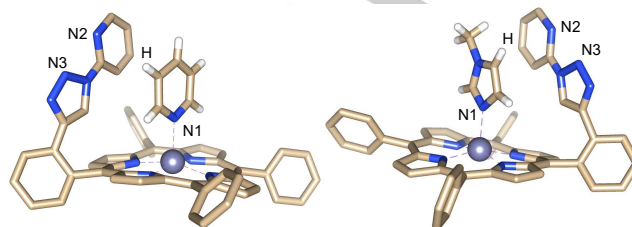
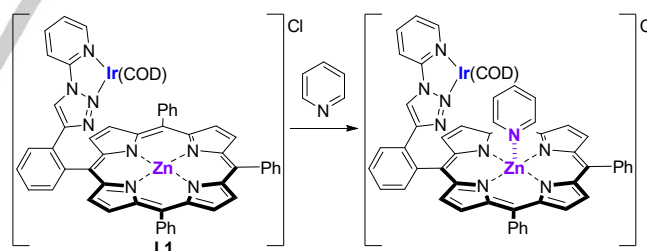


**Figure 2.** X-ray structures of the supramolecular assemblies between ligand **L** and pyridine (left) as well as *N*-methylimidazole (right) [capped sticks representation except the zinc atom that is ball representation, hydrogen atoms have been omitted except those from the nitrogen-containing substrates]. Color code: carbon (brown), nitrogen (blue), hydrogen (white). Selected distances [Å]:  $\text{Zn}\cdots\text{N1}$  2.14,  $\text{H}\cdots\text{N2}$  3.54,  $\text{H}\cdots\text{N3}$  3.92 (left) and  $\text{Zn}\cdots\text{N1}$  2.09,  $\text{H}\cdots\text{N2}$  3.79,  $\text{H}\cdots\text{N3}$  3.95 (right).

In parallel, coordination chemistry studies by  $^1\text{H}$  NMR and HRMS ( $m/z = 1121.2599$ ) showed that the reaction between **L** and 0.5 equivalents of  $[\text{Ir}(\text{COD})(\text{Cl})_2]$  afforded the corresponding cationic iridium complex **L1** (**Scheme 2**, see **Figures S8-S10**).<sup>[18]</sup> Subsequent  $^1\text{H}$  NMR studies by treatment of the iridium complex **L1** with increasing amounts of pyridine showed a single set of up-field shifted protons belonging to pyridine (**Scheme 2**) in a similar way as it was observed with the titration studies between **L** and pyridine (see **Figures S11-S12**).<sup>[18]</sup>



**Scheme 2.** Simultaneous coordination of both iridium and pyridine to **L**.

Having established that **L** enables the binding of pyridine inside the zinc(II)-porphyrin pocket simultaneously to the coordination of the *N,N*-chelating unit towards the potentially, catalytically active iridium center, we embarked in the catalytic assessment of **L** as a supramolecular ligand in iridium-catalyzed C-H bond borylations between unfunctionalized pyridine and bis(pinacolato)diboron ( $\text{B}_2\text{pin}_2$ ) as a model reaction (**Table 1**). This reaction is well-known to give a mixture of *meta*- and *para*-borylated products with classical bipyridine ligands<sup>[15a]</sup> and it represents a benchmark test for evaluating the activity and the regio-selectivity outcome.<sup>[13]</sup> Initially, we screened solvents that

## RESEARCH ARTICLE

were known to be used in iridium catalyzed C-H bond borylation of (hetero)arenes such as heptane and ethers at temperatures near to their boiling point.<sup>[10-15,22]</sup> Although poor conversions were observed, an exquisite *meta* selectivity was evidenced as only the products resulting from *mono*- and *bis*-borylation **1** and **2** formed without any detectable *para* or *ortho* regioisomers **3** or **4** (Table 1, entries 1-4). The reaction in toluene as solvent at 70 °C revealed as the optimal one for obtaining the *mono*-functionalized product with *meta* selectivity in an isolated yield of 54% (Table 1, entry 5, GC-yield 90%).<sup>[23]</sup> This is rather unexpected because non-functionalized arenes (i.e. toluene) are typically more reactive than pyridine using bipyridine- or phenantroline-derived ligands for iridium-catalyzed C-H bond borylation reactions.<sup>[13,22,24]</sup> In our case, we only detected trace amounts of borylated toluene and up to 15% (based on B<sub>2</sub>pin<sub>2</sub>) in the case of the reaction performed at higher 80 °C, that again exhibited excellent *meta*-selectivity for the C-H bond borylation of pyridine (Table 1, entry 6). For instance, with 58 times more toluene than pyridine in the reaction mixture, our supramolecular catalyst exhibits a high preference for the pyridine substrate than for the aromatic toluene one with an overall selectivity *S* estimated at 380 for the most unfavorable scenario.<sup>[25]</sup> Decreasing the temperature to 60 °C completely inhibited the catalysis (Table 1, entry 7). This suggests that the substrate-catalyst or product-catalyst binding via Zn<sup>II</sup>⋯N coordination is strong and it only becomes reversible to enable turnovers in catalysis at higher temperatures.<sup>[26]</sup> Switching the toluene solvent for a more bulky *p*-xylene led to no borylation at the solvent and high reactivity towards *meta*-selectivity in only 12 hours (Table 1, entry 8). Doubling the amounts of both B<sub>2</sub>pin<sub>2</sub> and the iridium catalyst led to the bis-borylated, *meta*-selective product **2** in an isolated yield of 70% (Table 1, entry 9), which represents the best result so far obtained for bis-functionalization to date.<sup>[27]</sup> The fact that aromatic apolar solvents such as toluene or *p*-xylene are crucial for the activity and selectivity of the catalysis, indirectly indicates that the polar ones (i.e. ethers) significantly disturb the binding of the substrate to the ligand **L**.<sup>[28]</sup> A similar reasoning may explain the higher reactivity encountered when using [Ir(COD)(Cl)]<sub>2</sub> instead of the typically more reactive [Ir(COD)(OMe)]<sub>2</sub><sup>[9-13,15,17,22-24]</sup> as the released methoxide anion from the former could bind to the zinc(II) center in **L** (Table 1, entry 2). The reactions performed in the absence of iridium or in the absence of ligand **L**, respectively, led to no conversion of pyridine substrate (see Table S1).<sup>[18]</sup>

**Table 1.** Reaction optimization for the iridium-catalyzed C-H bond borylation of pyridine.<sup>[a]</sup>

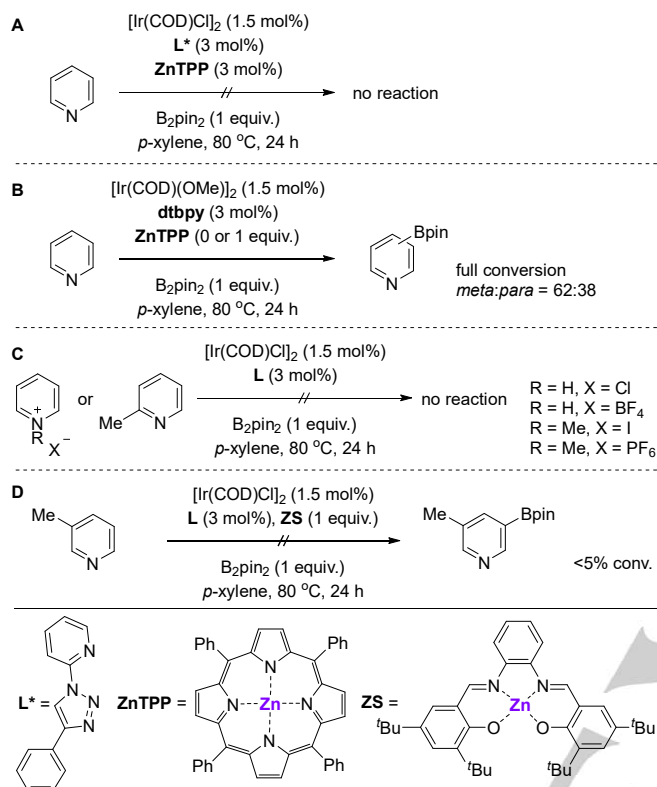
Entry	Solvent	T (°C)	t (h)	Conv. (%) <sup>[b]</sup>	(1+2):3:4 <sup>[c]</sup>	1:2 <sup>[d]</sup>
1	heptane	80	48	30	100:0:0	90:10
2 <sup>[e]</sup>	heptane	80	48	21	100:0:0	100:0
2	THF	50	48	0	-	-
3	MTBE	80	48	33	100:0:0	89:11
4	2-MeTHF	80	24	17	100:0:0	100:0
5	toluene	70	24	>99 (54) <sup>[f]</sup>	100:0:0	90:10
6	toluene	80	24	>99	100:0:0	25:75
7	toluene	60	24	<5	-	-
8	<i>p</i> -xylene	80	12	>99	100:0:0	40:60
9 <sup>[g]</sup>	<i>p</i> -xylene	80	48	>99 (70) <sup>[f]</sup>	100:0:0	13:87

[a] Reaction conditions: pyridine (0.162 mmol), B<sub>2</sub>pin<sub>2</sub> (0.162 mmol), [Ir(COD)(Cl)]<sub>2</sub> (1.5 mol%), **L** (3 mol%), solvent (1 mL). [b] Conversion determined as pyridine consumption. [c] Ratio *meta/para/ortho* functionalization of pyridine determined by <sup>1</sup>H NMR and GC using *n*-dodecane as internal standard. [d] Ratio *mono/bis*-functionalization of the *meta*-borylated product determined by <sup>1</sup>H NMR and GC-MS using *n*-dodecane as internal standard. [e] Reaction performed with [Ir(COD)(OMe)]<sub>2</sub> instead of [Ir(COD)(Cl)]<sub>2</sub>. [f] Isolated yield of the main product displayed in brackets. [g] Reaction performed with 3 equivalents of B<sub>2</sub>pin<sub>2</sub>, 3 mol% of [Ir(COD)(Cl)]<sub>2</sub> and 6 mol% of **L**.

To further rationalize the origin of this high *meta*-selectivity for the iridium-catalyzed C-H bond borylation reaction, a number of control experiments were performed (Scheme 3). First, the catalysis was attempted replacing the supramolecular ligand **L** for the individual components forming it, that is, zinc(II)-tetraphenylporphyrin (**ZnTPP**) and the *N,N*-chelating ligand **L**\* (Scheme 3A). Under the standard reaction conditions, the starting material pyridine was fully recovered unreacted, highlighting the relevance of covalently-linking the substrate recognition site to the catalytically active site as it is the case in the supramolecular ligand **L**. For comparison purposes, the reaction performed using 4,4'-di-*tert*-butyl-2,2'-dipyridyl (**dtbpy**) as ligand with or without the presence of **ZnTPP** led to an almost statistical mixture of *meta*- and *para*-borylated products (Scheme 3B).<sup>[15a]</sup> The relevance of the substrate binding to the zinc(II)-porphyrin pocket was further evidenced by the lack of reactivity observed for pyridines having no lone pair available for binding (i.e. pyridinium derivatives, Scheme 3C) as well as for pyridines unable to bind to the zinc atom due to steric shields (i.e. 2-methylpyridine, Scheme 3C).<sup>[28,29]</sup> A last experiment was performed adding to the standard reaction conditions zinc(II)-salphen (**ZS**) as a substrate competitive inhibitor (Scheme 3D) since it is known that zinc(II)-salphen derivatives bind to pyridine derivatives typically two orders of magnitude higher than zinc(II)-porphyrins.<sup>[28a,30]</sup> In this scenario, an almost complete inhibition of

## RESEARCH ARTICLE

catalysis took place with one equivalent of **ZS**. These observations show that the substrate is significantly bound to the zinc(II)-salphen **ZS** in which no catalysis takes place and that the catalysis do occur only if the substrate binds to the supramolecular ligand **L**.

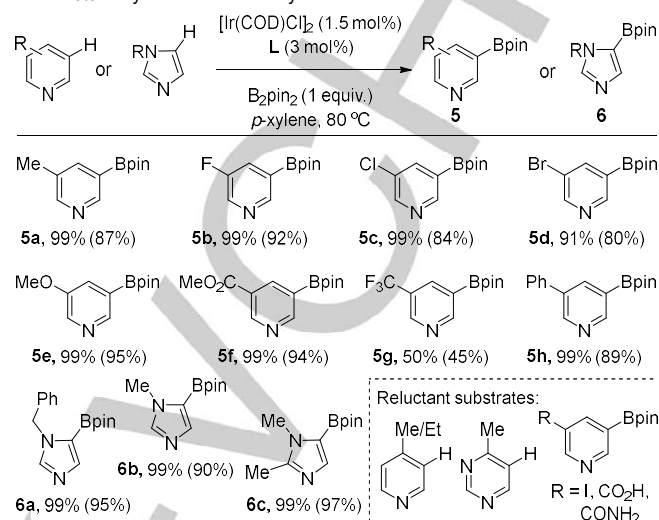


**Scheme 3.** Control experiments.

Next, a substrate scope was evaluated. The supramolecular catalytic system was found compatible with 3-substituted pyridine derivatives giving the respective *meta*-borylated products in yields up to 99% (**Table 2**). For instance, alkyl, aryl, ether, ester, and halogen (F, Cl, Br, CF<sub>3</sub>, except iodide) functionalities were tolerated (**5a–5h**, **Table 2**). On the other hand, no reactivity was observed for carboxylic acid or amide groups (**Table 2**). 5-membered ring heterocycles such as *N*-protected imidazoles delivered the  $\beta$ -substituted borylated products in virtually quantitative yields (**6a–6c**), which appears promising with respect to literature precedents.<sup>[31]</sup> Additionally, semi-empirical molecular modelling (PM3-level) showed that the supramolecular iridium catalyst fits well also for the  $\beta$ -C-H bond selectivity observed for 5-membered ring heterocycles (see Figure S15). Interestingly, the 2-methylimidazole substrate which is known to bind to zinc(II)-porphyrinoids derivatives<sup>[32]</sup> did afford the corresponding  $\beta$ -C-H bond borylated derivative **6c** in 97% isolated yield. This strikingly contrast with the lack of reactivity found for 2-methylpyridine (**Scheme 3C**) and it clearly shows that the geometry of the substrate is a key parameter for the reactivity observed within this supramolecular catalyst. Limitations of the catalytic system appeared when considering 4-substituted pyridines and

pyrimidines which did not react due to steric effects as it was noted elsewhere (**Table 2**).<sup>[33]</sup>

**Table 2.** Substrate evaluation for the supramolecular iridium-catalyzed C-H bond *meta*-borylation controlled by remote Zn...N interactions.<sup>[a]</sup>



[a] Yields estimated by GC analysis and isolated yields shown in brackets, the slight difference in these values is due to loss and/or partial protodeboration of the products during purification.

We then embarked on the kinetic evaluation of this supramolecular catalysis with a model reaction using 3-methylpyridine as the substrate.<sup>[18]</sup> For this purpose, preliminary reaction progress kinetic analysis (RPKA) were carried out at same and different excess concentrations (see Section 5.4 in the Supporting Information).<sup>[34]</sup> As it was found before,<sup>[17b]</sup> the reaction features an incubation period that depends on the catalyst loading, being shorter at higher catalyst loadings (**Figure 3**, left). In addition, we noted that at lower concentrations of B<sub>2</sub>pin<sub>2</sub>, its consumption was not directly correlated to the formation of the product as it is the case when considering the 3-methylpyridine substrate consumption (**Figure 3**, middle). Higher reaction rates have been observed with B<sub>2</sub>pin<sub>2</sub> instead of HBpin for a certain types of substrates.<sup>[15b]</sup> This suggests, that a second catalytic cycle is operating to some extent involving a degradation side-product from B<sub>2</sub>pin<sub>2</sub>, probably HBpin because H<sub>2</sub> (another side-product)<sup>[35,36]</sup> is detected by <sup>1</sup>H NMR spectroscopy studies.<sup>[18]</sup> Besides these observations, the RPKA analysis showed that the catalysis is first order in iridium and pseudo-zero-order in B<sub>2</sub>pin<sub>2</sub>, as it could be expected.<sup>[15b,17a]</sup> On the other hand, the order in substrate did not match to zero as shown by Hartwig with a non-supramolecular catalyst,<sup>[15b]</sup> but it rather fitted to a pseudo-first order as it has been seen with non-heteroaromatic substrates.<sup>[17a]</sup> This strongly supports that the resting state in this supramolecular catalysis does not involve an iridium complex coordinated to the *N*-containing substrate *via* Ir-N bonding such as **Ir-1** (**Figure 1B**),<sup>[15b]</sup> but rather a tris-boryl iridium species formed later in the catalytic cycle likely upon substrate binding to the zinc(II)-porphyrin site such as **A** (**Scheme 4**). Although the overlay was not fully precise by RPKA analysis due to the limitations previously described, unambiguous catalyst deactivation was evidenced that we ascribed to catalyst degradation<sup>[37]</sup> as no

## RESEARCH ARTICLE

product inhibition was observed by RPKA analysis.<sup>[18]</sup> This indicates that the catalyst immediately releases the product after formation in a similar way as enzymes do. We anticipate that the bulkiness of the product might be at the origin for the absence of product inhibition, thus indirectly enhancing substrate binding under catalytic conditions. Consequently, such catalytic system may follow an enzymatic Michaelis-Menten kinetic behavior in

which the whole catalytic events occur upon binding of the substrate in the zinc(II)-porphyrin pocket (**Figure 3**, right). In fact, a decent fitting ( $R^2 = 0.994$ ) was found for the plot of rate versus concentration of 3-methylpyridine substrate with  $V_{\max} = 0.104 (\pm 0.02) \text{ M h}^{-1}$  and  $K_{\text{mm}} = 0.107 (\pm 0.04) \text{ M}$ .

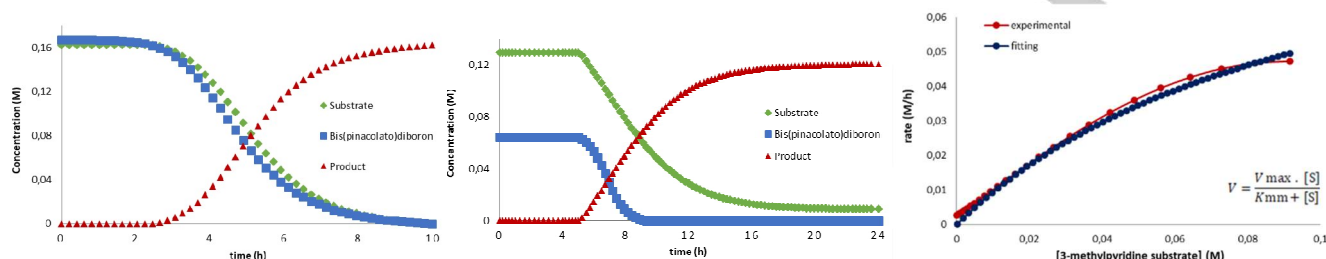
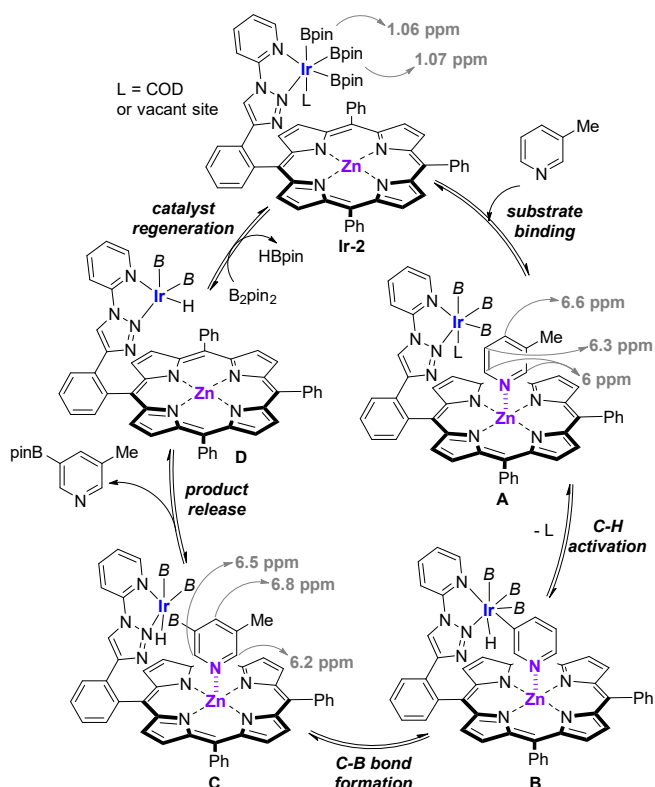


**Figure 3.** Graphical representation of the kinetic profiles under standard (stoichiometric) reaction conditions (left; [3-methylpyridine] = 0.162 M, [B<sub>2</sub>pin<sub>2</sub>] = 0.162 M) and under half concentration of B<sub>2</sub>pin<sub>2</sub> with respect to the substrate (middle; [3-methylpyridine] = 0.130 M, [B<sub>2</sub>pin<sub>2</sub>] = 0.065 M); and graphical representation of the reaction rate versus substrate concentration plots together with the fitting to the Michaelis-Menten rate equation (right).

Aiming at identifying potential catalytically active species, the *meta*-C-H bond borylation reaction was followed on time under catalytic conditions using multinuclei NMR spectroscopy (**Scheme 4**). First, the pre-active iridium catalyst **Ir-2** involving trisboryl species was identified at catalytically-relevant temperatures (see Section 6 in the Supporting Information).<sup>[18]</sup> The <sup>1</sup>H NMR studies of **Ir-2** showed two set of signals at  $\delta = 1.07$  and 1.06 ppm corresponding to two different set of Bpin groups in a 1:2 ratio (one Bpin fragment was in axial position and the other two Bpin fragments were in equatorial position; *note that they are not equivalent at high temperatures due to the low symmetry of the species*).<sup>[17a]</sup> Similar observations were evidenced by <sup>11</sup>B NMR studies ( $\delta = 22$  and 23 ppm in a 1:2 ratio).<sup>[18]</sup> Next, the reaction between 3-methylpyridine and B<sub>2</sub>pin<sub>2</sub> with the *in situ* formed **Ir-2** was followed on time.<sup>[18]</sup> The 3-methylpyridine substrate was bound to the supramolecular ligand **L** via Zn⋯N interaction under catalytic conditions as regards of the up-field shifted pyridine proton signals strongly supporting the formation of species **A** (**Scheme 4**). Although the transient iridium-hydride species **B** (as well as **D**) was not detected, the product-to-catalyst species **C** was formed according to the disappearance of the pyridine signals belonging to **A** and the merger of a set of three new up-field shifted pyridine proton signals (**Scheme 4**). Further GC analysis and <sup>1</sup>H NMR spectroscopy studies indicated quantitative formation of *meta*-borylated product, indicating that the product is easily released from the catalyst pocket under the catalytic conditions. The overall combination of above-described results together with previous data from the literature,<sup>[38]</sup> enabled us to propose a catalytic cycle in which all the reaction steps occur after substrate binding to the porphyrin pocket of **L** with final release of the product after selective *meta*-C-H bond borylation (**Scheme 4**).

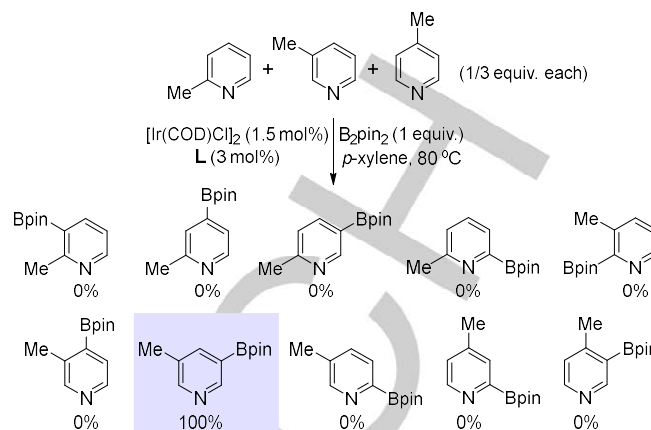
## RESEARCH ARTICLE



**Scheme 4.** Postulated reaction mechanism for the supramolecular iridium-catalyzed C-H bond *meta*-borylation of pyridines using **L**. **B** = (pinacolato)boron. The ppm values refer to the proton signals from the pyridine C-H bonds pointed out by the gray arrows that were determined by  $^1\text{H}$  NMR spectroscopy at 80 °C under catalytic conditions.

To further show the enzyme-like behavior of this supramolecular iridium catalyst, we wondered whether it would be possible to perform substrate-selective catalysis with a reaction comprising a mixture of all three possible regioisomers derived from 3-methylpyridine as the substrates.<sup>[39]</sup> Indeed, the supramolecular catalyst formed upon combination of the iridium precursor and **L** gave a selective system towards the exclusive *meta*-selective borylation of the *meta* isomer with no reactivity observed at the other substrates even upon 24 hours reaction time (**Scheme 5**). A single product formed out of the 10 possible ones considering the different regio- and site-selectivities. Thus, the system leads to substrate-selectivity maintaining an exquisite level of regio-selectivity as well.

Finally, we studied the ability of this supramolecular iridium catalyst to display dormant reactivity in a way that the borylation only occurs when an external stimuli is applied to the system. More precisely, and considering the lack of reactivity of pyridinium salts (*vide supra*), we decided to introduce after 3 hours of reaction time one equivalent of *N,N*-diisopropylethylamine base (DIPEA) as an external chemical stimuli with the hope that an *in situ* deprotonation of the substrate will bring the pyridine to bind the zinc pocket of the supramolecular ligand **L** following iridium-catalyzed remote borylation. Indeed, we were pleased to detect 90% conversion of pyridine after 16 h according to the above described reaction design (**Figure 4**).



**Scheme 5.** Substrate-selectivity targeted using the supramolecular iridium catalyst featuring secondary Zn...N interactions.

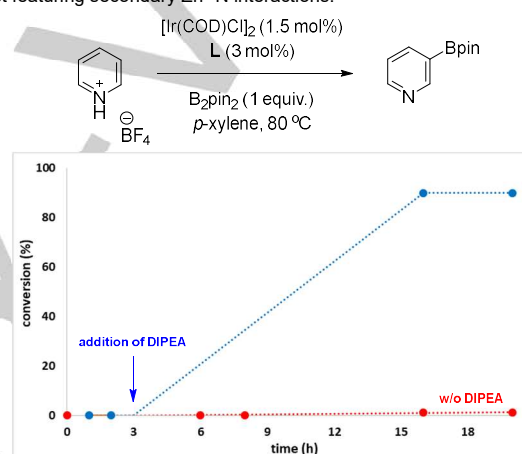


**Figure 4.** Dormant reactivity featured by the supramolecular iridium catalyst using a base (DIPEA) as an external chemical stimuli.

## Conclusion

In summary, we have reported a rationally-designed supramolecular borylating iridium catalyst displaying C-H bond *meta*-selectivity for challenging pyridine-like derivatives *via* reversible and dynamic Zn...N binding.<sup>[16]</sup> The predictability of the selectivity was made possible considering the relatively strong association constant between the substrates and the catalyst and the precise distance between the active site and the recognition site supported by a straightforward combination of experimental and theoretical (semi-empirical) studies. The catalytic system displayed unique enzymatic features as regards of the kinetics, mechanism and substrate-selectivity herein presented. The incorporation of substrate-recognition sites based on zinc(II)-porphyrin scaffolds in the second coordination sphere of a *priori* inactive or unselective catalytic moieties clearly constitutes an alternative to the more classical fine-tuning at the first coordination sphere. In addition, we showed that *N,N*-chelating ligands beyond bipyridine or phenanthroline derivatives are suitable for iridium-catalyzed C-H bond borylations.<sup>[40]</sup> Because this presented approach is readily tunable at the active site and the substrate-recognition site, other types of transition metal-

## RESEARCH ARTICLE

catalyzed transformations towards unbiased substrates could be envisioned as well as exploiting them for temporal control of reactivity considering the preliminary dormant reactivity studies.

## Acknowledgements

The research leading to these results has received funding from the People Programme (Marie Curie Actions) of the European Union's Seventh Framework Programme (FP7/2007-2013) under REA grant agreement n. PCOFUND-GA-2013-609102, through the PRESTIGE programme coordinated by Campus France (P.Z.). Financial support from ANR-JCJC (PhD grant to J.T.), Fondation Rennes 1 (MSc grant to S.A.-S.), CNRS, Universite de Rennes 1, Rennes Metropole, and Region Bretagne (Strategie d'Attractivite Durable and Boost'Europe) is acknowledged.

**Keywords:** iridium • pyridine • porphyrinoids • homogeneous catalysis • supramolecular chemistry

- [1] a) C-H Activation in *Topics in Current Chemistry* (Eds.: J.-Q. Yu, Z. Shi), Springer-Verlag, Berlin-Heidelberg, **2010**; b) R. Shang, L. Ilies, E. Nakamura, *Chem. Rev.* **2017**, *117*, 9086-9139; c) Y. Yang, J. Lan, J. You, *Chem. Rev.* **2017**, *117*, 8787-8863; d) L. McMurray, F. O'Hara, M. J. Gaunt, *Chem. Soc. Rev.* **2011**, *40*, 1885-1898; e) R. R. Karimov, J. F. Hartwig, *Angew. Chem. Int. Ed.* **2018**, *57*, 4234-4241; f) J. Yamaguchi, A. D. Yamaguchi, K. Itami, *Angew. Chem. Int. Ed.* **2012**, *51*, 8960-9009.
- [2] a) K. M. Engle, T.-S. Mei, M. Wasa, J.-Q. Yu, *Acc. Chem. Res.* **2012**, *45*, 788-802; b) X.-S. Xue, P. Ji, B. Zhou, J.-P. Cheng, *Chem. Rev.* **2017**, *117*, 8622-8648.
- [3] a) C. Sambiagio, D. Schönbauer, R. Blicke, T. Dao-Huy, G. Pototschnig, P. Schaaf, T. Wiesinger, M. F. Zia, J. Wencel-Delord, T. Besset, B. U. W. Maes, M. Schnürch, *Chem. Soc. Rev.* **2018**, *47*, 6603-6743; b) S. Rej, Y. Ano, N. Chatani *Chem. Rev.* **2020**, *120*, 1788-1887; c) G. Meng, N. Y. S. Lam, E. L. Lucas, T. G. Saint-Denis, P. Verma, N. Chekshin, J.-Q. Yu, *J. Am. Chem. Soc.* **2020**, *142*, 10571-10591; d) R.-Y. Zhu, M. E. Farmer, Y.-Q. Chen, J.-Q. Yu, *Angew. Chem. Int. Ed.* **2016**, *55*, 10578-10599.
- [4] a) D. L. Davies, S. A. Macgregor, C. L. McMullin, *Chem. Rev.* **2017**, *117*, 8649-8709; b) L. Ackermann, *Chem. Rev.* **2011**, *111*, 1315-1345.
- [5] a) N. Della Ca', M. Fontana, E. Motti, M. Catellani, *Acc. Chem. Res.* **2016**, *49*, 1389-1400; b) D. Lichosyt, Y. Zhang, K. Hurej, P. Dydio, *Nat. Catal.* **2019**, *2*, 114-122.
- [6] a) D. Ringe, G. A. Petsko, *Science* **2008**, *320*, 1428-1429; b) *From enzyme models to model enzymes* (Eds.: A. J. Kirby, F. Hollfelder), RSC, London, **2009**.
- [7] a) A. Warshel, P. K. Sharma, M. Kato, Y. Xiang, H. Liu, M. H. M. Olsson, *Chem. Rev.* **2006**, *106*, 3210-3235; b) G. G. Hammes, S. J. Benkovic, S. Hammes-Schiffer, *Biochemistry* **2011**, *50*, 10422-10430.
- [8] a) *Supramolecular Catalysis* (Ed.: P. W. N. M. van Leeuwen), Wiley-VCH, Weinheim, **2008**; b) M. J. Wiestner, P. A. Ulmann, C. A. Mirkin, *Angew. Chem. Int. Ed.* **2011**, *50*, 114-137; c) M. Raynal, P. Ballester, A. Vidal-Ferran, P. W. N. M. van Leeuwen, *Chem. Soc. Rev.* **2014**, *43*, 1660-1733; d) M. Raynal, P. Ballester, A. Vidal-Ferran, P. W. N. M. van Leeuwen, *Chem. Soc. Rev.* **2014**, *43*, 1734-1787; e) J. Meeuwissen, J. N. H. Reek, *Nat. Chem.* **2010**, *2*, 615-621; f) P. Dydio, J. N. H. Reek *Chem. Sci.* **2014**, *5*, 2135-2145; g) H. J. Davis, R. J. Phipps, *Chem. Sci.* **2017**, *8*, 864-877; h) J. Trouve, R. Gramage-Doria, *Chem. Soc. Rev.* **2021**, doi:10.1039/D0CS01339K.
- [9] Y. Kuninobu, T. Torigoe, *Org. Biomol. Chem.* **2020**, *18*, 4126-4134.
- [10] a) Y. Kuninobu, H. Ida, M. Nishi, M. Kanai, *Nat. Chem.* **2015**, *7*, 712-717; b) J. Zeng, M. Naito, T. Torigoe, M. Yamanaka, Y. Kuninobu, *Org. Lett.* **2020**, *22*, 3485-3489; c) S.-T. Bai, C. B. Bheeter, J. N. H. Reek, *Angew. Chem. Int. Ed.* **2019**, *58*, 13039-13043; d) J. Wang, T. Torigoe, Y. Kuninobu, *Org. Lett.* **2019**, *21*, 1342-1346; e) X. Lu, Y. Yoshigoe, H. Ida, M. Nishi, M. Kanai, Y. Kuninobu, *ACS Catal.* **2019**, *9*, 1705-1709.
- [11] a) H. J. Davis, M. T. Mihai, R. J. Phipps, *J. Am. Chem. Soc.* **2016**, *138*, 12759-12762; b) G. R. Genov, J. L. Douthwaite, A. S. K. Lahdenpera, D. C. Gibson, R. J. Phipps, *Science* **2020**, *367*, 1246-1251; c) J. R. Montero Bastidas, T. J. Oleskey, S. L. Miller, M. R. Smith, R. E. Maleczka, *J. Am. Chem. Soc.* **2019**, *141*, 15483-15487; d) M. T. Mihai, B. D. Williams, R. J. Phipps, *J. Am. Chem. Soc.* **2019**, *141*, 15477-15482; e) B. Lee, Bernadette, M. T. Mihai, V. Stojalnikova, R. J. Phipps, *J. Org. Chem.* **2019**, *84*, 13124-13134; f) M. T. Mihai, H. J. Davis, G. R. Genov, R. J. Phipps, *ACS Catal.* **2018**, *8*, 3764-3769; g) M. E. Hoque, R. Bisht, C. Haldar, B. Chattopadhyay, *J. Am. Chem. Soc.* **2017**, *139*, 7745-7748; h) W. A. Golding, R. J. Phipps, *Chem. Sci.* **2020**, *11*, 3022-3027; i) R. Bisht, M. E. Hoque, B. Chattopadhyay, *Angew. Chem. Int. Ed.* **2018**, *57*, 15762-15766; j) B. Chattopadhyay, J. E. Dannatt, I. L. Andujar-De Sanctis, K. A. Gore, R. E. Maleczka, D. A. Singleton, M. R. Smith, *J. Am. Chem. Soc.* **2017**, *139*, 7864-7871.
- [12] a) L. Yang, N. Uemura, Y. Nakao, *J. Am. Chem. Soc.* **2019**, *141*, 7972-7979; b) L. Yang, K. Semba, Y. Nakao, *Angew. Chem. Int. Ed.* **2017**, *56*, 4853-4857.
- [13] a) Y. Kuroda, Y. Nakao, *Chem. Lett.* **2019**, *48*, 1092-1100; b) C. Haldar, M. E. Hoque, R. Bisht, B. Chattopadhyay, *Tetrahedron Lett.* **2018**, *59*, 1269-1277; c) K. Murakami, S. Yamada, T. Kaneda, K. Itami, *Chem. Rev.* **2017**, *117*, 9302-9332.
- [14] a) A. Ros, R. Fernández, J. M. Lassaletta, *Chem. Soc. Rev.* **2014**, *43*, 3229-3243; b) *Boronic Acids. Preparation, Applications in Organic Synthesis*, (Ed.: D. G. Hall), Wiley-VCH, Weinheim, **2011**; c) E. C. Neeve, S. J. Geier, I. A. I. Mkhalid, S. A. Westcott, T. B. Marder, *Chem. Rev.* **2016**, *116*, 9091-9161; d) M. Wang, Z. Shi, *Chem. Rev.* **2020**, *120*, 7348-7398.
- [15] a) J. Takagi, K. Sato, J. F. Hartwig, T. Ishiyama, N. Miyaura, *Tetrahedron Lett.* **2002**, *43*, 5649-5651; b) M. A. Larsen, J. F. Hartwig, *J. Am. Chem. Soc.* **2014**, *136*, 4287-4299.
- [16] For pioneering findings on kinetically labile Zn-N interactions for purely organic reactions, see: a) R. P. Bonar-Law, L. G. Mackay, C. J. Walter, V. Marvaud, J. K. M. Sanders, *Pure Appl. Chem.* **1994**, *66*, 803-810; b) J. K. M. Sanders, *Pure Appl. Chem.* **2000**, *72*, 2265-2274. The uniqueness of Zn<sup>2+</sup> over other cations for metal catalysis have been studied in reference 28.
- [17] The active catalytic species in iridium-catalyzed C-H bond borylation is postulated to be a N,N-chelated iridium trisboryl complex, for seminal works see: a) T. M. Boller, J. M. Murphy, M. Hapke, T. Ishiyama, N. Miyaura, J. F. Hartwig, *J. Am. Chem. Soc.* **2005**, *127*, 14263-14278; b) T. Ishiyama, J. Takagi, K. Ishida, N. Miyaura, N. R. Anastasi, J. F. Hartwig, *J. Am. Chem. Soc.* **2002**, *124*, 390-391; c) C. W. Liskey, C. S. Wei, D. R. Pahls, J. F. Hartwig, *Chem. Commun.* **2009**, 5603-5605.
- [18] For details, see the supporting information.
- [19] P. Thordarson, *Chem. Soc. Rev.* **2011**, *40*, 1305-1323.
- [20] a) X. Zhang, K. N. Houk, *Acc. Chem. Res.* **2005**, *38*, 379-385; b) K. N. Houk, A. G. Leach, S. P. Kim, X. Zhang, *Angew. Chem. Int. Ed.* **2003**, *42*, 4872-4897.
- [21] CCDC 2061921-2061922 contain the supplementary crystallographic data for this paper. These data are provided free of charge by The Cambridge Crystallographic Data Centre.
- [22] a) T. Ishiyama, Y. Nobuta, J. F. Hartwig, N. Miyaura, *Chem. Commun.* **2003**, 2924-2925; b) R. J. Oeschger, M. A. Larsen, A. Bismuto, J. F. Hartwig, *J. Am. Chem. Soc.* **2019**, *141*, 16479-16485; see reference 15b.
- [23] A similar conversion and yield was obtained under extensive ligand optimization in dioxane at room temperature, see reference 12a.
- [24] a) T. Ishiyama, J. Takagi, J. F. Hartwig, N. Miyaura, *Angew. Chem. Int. Ed.* **2002**, *41*, 3056-3058; b) T. Ishiyama, J. Takagi, Y. Yonekawa, J. F. Hartwig, N. Miyaura, *Adv. Synth. Catal.* **2003**, *345*, 1103-1106.
- [25] a) A. F. Schmidt, A. A. Kurokhtina, E. V. Larina, *Catal. Sci. Technol.* **2014**, *4*, 3439-3457; b) 1 mL of toluene as solvent corresponds to 9.4 mmol, as such, in the case of 15% borylation of toluene, the following

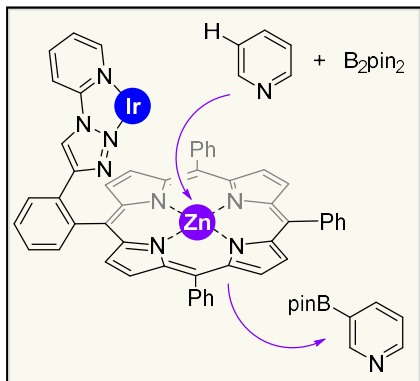
## RESEARCH ARTICLE

- formula for the overall selectivity is applied according to reference 24a:  
$$S = \frac{(n_{1+2}/n_{\text{pyridine}})/(n_{\text{borylated toluene}}/n_{\text{toluene}})}{[(0.162 \times 0.99)/0.162]/[(0.162 \times 0.15)/9.4]} = 381.$$
- [26] <sup>1</sup>H NMR studies at room temperature show that both pyridine derivatives (substrates) and borylated ones (products) bind to **L** alternatively in a fast exchange at the NMR time scale. For details, see the supporting information. However, it cannot be ruled out that other inactive pathways are operating at 60 °C.
- [27] 16% of isolated bis-borylated product **2** was obtained according to reference 12a.
- [28] O-containing polar solvents (DMF, DMSO, acetone, THF, etc.) completely cleave the Zn...N interaction between zinc(II)-porphyrinoids and pyridine derivatives, for examples see references: a) M. Kadri, J. Hou, V. Dorcet, T. Roisnel, L. Bechki, A. Miloudi, C. Bruneau, R. Gramage-Doria, *Chem. Eur. J.* **2017**, *23*, 5033-5043; b) P. Zardi, T. Roisnel, R. Gramage-Doria, *Chem. Eur. J.* **2019**, *25*, 627-634.
- [29] For selected examples of negligible binding between 2-substituted pyridines and zinc(II)-porphyrinoids, see: a) M. Morisue, T. Morita, Y. Kuroda, *Org. Biomol. Chem.* **2010**, *8*, 3457-3463; b) J. S. Summers, A. M. Stolzenberg, *J. Am. Chem. Soc.* **1993**, *115*, 10559-10567; c) C. H. Kirksey, P. Hambright, C. B. Storm, *Inorg. Chem.* **1969**, *8*, 2141-2144; and reference 27.
- [30] a) A. L. Singer, D. A. Atwood, *Inorg. Chim. Acta* **1998**, *277*, 157-162; b) G. A. Morris, H. Zhou, C. L. Stern, S. T. Nguyen, *Inorg. Chem.* **2001**, *40*, 3222-3227; c) A. W. Kleij, M. Lutz, A. L. Spek, P. W. N. M. van Leeuwen, J. N. H. Reek, *Chem. Commun.* **2005**, 3661-3663; d) A. W. Kleij, M. Kuil, D. M. Tooke, M. Lutz, A. L. Spek, J. N. H. Reek, *Chem. Eur. J.* **2005**, *11*, 4743-4750.
- [31] M. R. Smith III, R. E. Maleczka, Jr., A. K. Venkata, E. Onyeozili, *Process for Producing Oxazole, Imidazole, Pyrazole Boryl Compounds*, US Pat. 7,709,654B2, **2008**.
- [32] For selected examples of binding between 2-methylimidazole and zinc(II)-porphyrinoids, see: a) M. Nappa, J. S. Valentine, *J. Am. Chem. Soc.* **1978**, *100*, 5075-5080; b) K. M. Kadish, L. R. Shiue, R. K. Rhodes, L. A. Bottomley, *Inorg. Chem.* **1981**, *20*, 1274-1277.
- [33] S. A. Sadler, H. Tajuddin, I. A. I. Mkhaliid, A. S. Batsanov, D. Albesa-Jove, M. S. Cheung, A. C. Maxwell, L. Shukla, B. Roberts, D. C. Blakemore, Z. Lin, T. B. Marder, P. G. Steel, *Org. Biomol. Chem.* **2014**, *12*, 7318-7327.
- [34] D. G. Blackmond, *Angew. Chem. Int. Ed.* **2005**, *44*, 4302-4320.
- [35] The stoichiometric reaction between 3-methylpyridine and HBpin under our standard conditions led to 79% of borylated product and 15% of unreacted HBpin, indicating that B<sub>2</sub>pin<sub>2</sub> is a better borylating reagent than HBpin under our standard reaction conditions. Further details will be reported at due time.
- [36] Although we do not have any spectroscopical evidence for the formation of HBpin or any other borylated species derived from B<sub>2</sub>pin<sub>2</sub>, previous reports from the literature indicate that HBpin is indeed a borylating reagent with side-formation of H<sub>2</sub>, but less reactive than B<sub>2</sub>pin<sub>2</sub>, for details see: J. S. Wright, P. J. H. Scott, P. G. Steel, *Angew. Chem. Int. Ed.* **2021**, *60*, 2796-2821.
- [37] Attempts to isolate **L** after the catalysis indicate substantial degradation according to TLC analysis.
- [38] a) I. A. I. Mkhaliid, J. H. Barnard, T. B. Marder, J. M. Murphy, J. F. Hartwig, *Chem. Rev.* **2010**, *110*, 890-931; b) J. F. Hartwig, *Chem. Soc. Rev.* **2011**, *40*, 1992-2002; c) J. F. Hartwig, *Acc. Chem. Res.* **2012**, *45*, 864-873; d) L. Xu, G. Wang, S. Zhang, H. Wang, L. Wang, L. Liu, J. Jiao, P. Li, *Tetrahedron* **2017**, *73*, 7123-7157.
- [39] E. Lindback, S. Dawaigher, K. Warnmark, *Chem. Eur. J.* **2014**, *20*, 13432-13481.
- [40] R. L. Reyes, M. Sato, T. Iwai, K. Suzuki, S. Maeda, M. Sawamura, *Science* **2020**, *369*, 970-974.

## RESEARCH ARTICLE

## Entry for the Table of Contents

Insert graphic for Table of Contents here.



An iridium-based supramolecular catalyst (see figure) has been designed to selectively recognize pyridine-like derivative *via* secondary Zn $\cdots$ N interactions. Owing to the distance between the substrate binding site and the active site as well as the geometrical constraints, *meta*-selective borylation reactions were accomplished displaying catalytic behaviors typically encountered in enzymes.

Institute and/or researcher Twitter usernames: @INC\_CNRS @UnivRennes1 @Rafa\_gramage